JOURNAL OF OPTOELECTRONICS AND ADVANCED MATERIALS Vol. 12, No. 12, December 2010, p. 2391 - 2399

Electrochemical study of AISI 316L Stainless Steel in different nanoparticle suspensions

A.-M. CANTARAGIU*, G. CARAC[a], C. GHEORGHIES[b]
Faculty of Mechanics, Dunarea de Jos University, Galati, 800008, Romania
[a]Department of Chemistry, Faculty of Sciences, Dunarea de Jos University, Galati, 800008, Romania
[b]Department of Physics, Faculty of Sciences, Dunarea de Jos University, Galati, 800008, Romania

The aim of this paper is to study the corrosion behaviour of AISI 316L Stainless Steel (SS) in various solutions with nanoparticle suspensions by electrochemical testing. It is very important to determine the chemical reactivity of AISI 316L SS in the presence of some aqueous solutions in order to characterize the biocompatibility with the human body. The tested corrosive environments are: demineralised and deionised water at different immersion times, aqueous solution of 0.1 or 0.2 g/l TiO_2 as well as aqueous solution of 0.1 or 0.2 g/l Al_2O_3. The measurements at room temperature were made in a conventional three-electrodes chemical cell, using a platinum electrode, a calomel and an AISI 316 SS as working electrode. The corrosion process was examined by linear polarization (LP) using a Bio-Logic potentiostate. For the LP measurements the potential ranged between –1.15÷1.13 V vs. SCE. The immersion time before each measurement was 60 sec. to assess an equilibrium open potential. From the LP curves, the corrosion potential and parameters such as corrosion current, the polarisation resistance and corrosion rate are determined. Under certain circumstances, the results show that the nanoparticle suspensions act as a protective layer on the AISI 316L SS sample surface.

(Received November 3, 2010; accepted November 25, 2010)

Keywords: Stainless steel, Alumina, Titania, Corrosion rate, Polarization resistance

1. Introduction

The AISI 316L austenitic stainless steels find important and various applications such as construction materials in chemical and petrochemical industries, in oil and gas exploitation, shipbuilding, tanks and storage vessels for corrosive liquids, pharmaceutical, food and drug processing, in water purification and distribution systems, and in biomaterials industry. Its chief characteristics are superior corrosion, oxidation resistance [1-3] and good mechanical properties. The last of the above-mentioned industries industry cannot tolerate corrosion deposits in the manufactured product due to health-related reasons.

Materials (metals) are used mainly in the human body mainly for orthopaedic purposes and thus their degradation by corrosion must be negligible so that they can be used for various practical applications. The 316L Stainless Steel (316L SS) is frequently employed to prepare certain implant materials because of its low cost and acceptable biocompatibility [4]. The 316L SS is an improved version of 304 SS, with the addition of molybdenum and slightly higher nickel content. The resulting composition of 316L SS gives the steel a much increased corrosion resistance in many aggressive environments. For example, the molybdenum makes the steel more resistant to pitting and crevice corrosion in chloride-contaminated media, sea water and acetic acid vapours. The lower rate of general corrosion in mildly corrosive environments gives the steel a good atmospheric corrosion resistance in polluted marine atmospheres.

In recent years, nanoparticle thin films on metallic implant surfaces have received a great attention in the field of orthopaedics because of their excellent mechanical, osteoconductive and corrosion resistant properties [5]. It is well known that the composite coatings have a much greater corrosion resistance. The co-deposition of the nanoparticles is very effective due to their tribological properties and increasing availability. Among the nanomaterials, titania (TiO_2) and alumina (Al_2O_3) are in great demand for the generation of composite coating on steel with other metals or alloys [6,7]. Here, the nanoparticle corrosion effect is tested at different concentrations and exposure times. The corrosion process depends on material texture and topography. The temperature, composition of metallic substrates and electrolyte solution, size and concentration of suspension, immersion time are also influencing the surface resistance.

Currently, there are many methods to determine the corrosion rates of metals, such as gravimetric-based mass loss, quartz crystal microbalance-based mass loss, electrochemical, electrical resistance and solution analysis. The polarization measurement methods, based on electrochemical concepts, enable the determination of instantaneous reaction rates at electrode/solution interface, such as the corrosion current density in case of a corrosion system, from a single experiment. All other methods require multiple measurements over time in order to provide information on the corrosion rate [8].

There are two polarization-based measurement methods used to determine the corrosion rates: Tafel slopes extrapolation with corrosion potential [9-13] (Stern

method) and polarization resistance method (Stern and Geary method). However, it must be noted that polarization-based measurement method may imply error-producing factors such as diffusion limitation, high solution resistance, presence of competing red-ox reactions, and no uniform current and potential distributions, etc.

The aim of this work-paper is to evaluate the electrochemical behaviour of AISI 316L Stainless Steel in different nanoparticle suspensions by means of the linear polarization (LP) method. The results obtained by both polarization-based measurement methods could give the information about the influence of electrolyte solutions onto the metallic samples surface, the instantaneous corrosion rates, and to show the conditions and circumstances where the error-producing factors are important. These are possible due to the electrochemical parameters (the corrosion potential, E_{corr}, corrosion current, I_{corr}, polarisation resistance, R_p, corrosion rate, V_{corr}) automatically obtained from linear polarization curves.

2. Experimental research

2.1. Materials

Commercially available 316L SS specimens were used. The chemical composition as represented by ASTM A240 and ASME SA-240 specifications is indicated in the table below [3,5,14]. Before the electrochemical study, the samples were mechanically polished with fine grit SiC paper. Afterwards, the polished substrates were carefully chemically degreased with acetone and alcohol, and then rinsed with bi-distilled water before their immersion in the electrochemical cell.

Table 1. Chemical composition of AISI 316L stainless steel in mass fractions, wt%.

C	Mn	P	S	Si	Cr	Ni	Mo	Ti	Fe
0.020	1.70	0.04	0.01	0.30	18.00	12.00	2.50	0.20	65.23

Both chemical powders (TiO_2-Degussa P25 synthesis grade with the average size of 55 nm and Al_2O_3 with the size of 0.05 μm) were purchased from commercial sources and have the highest purity available. They were used without further purification. In order to analyse the corrosive behaviour of solutions on 316L SS surface, different electrolytes in various conditions were prepared. The experiments are carried out in demineralised and deionised water (real medium) in the absence and in the presence of nanoparticles. The corrosion effect of two types of concentrations (0.1 and 0.2 g/L) of TiO_2 and Al_2O_3 nanoparticles dissolved in water during three rates of time (1, 2 and 4 min.) was analysed.

2.2. Methods and instruments

A standard three electrode system (electrochemical cell from Pyrex glass) with a cell volume of 100 ml was used to perform the electrochemical investigations at room temperature. A disc-shaped working electrode, WE, was made of AISI 316L SS. The active area of the WE was 0.95 cm^2. An Hg_2Cl_2, saturated calomel electrode (SCE) served as the reference electrode (RE), and the counter electrode (CE) was a platinum sheet. The entire three-electrode assembly was placed in a Faraday cage to limit noise disturbance and then connected to the potentiostat/galvanostat The processes were carried out potentiodynamically (potential vs. current diagram) with a potentiostat/galvanostat model Bio-Logic SP-150 (France) interfaced with EC-Lab® Express V9.46 software for data acquisition and analysis. The choice of the measuring equipment, electrochemical recipient, CE and RE electrodes and the preparation of the WE were made in conformity with ASTM standards [15,16]. Before and after each experiment the pH and the electrical conductivity values were measured with a pH-meter model Consort C860 with 0.2% accuracy.

The corrosion process was examined by the LP method. Before each LP measurements, the open circuit potential (OCP) method was carried out in order to pre-polarize the electrochemical system. The immersion time is 60 sec. to assess the WE polarisation potential into the electrolytes solution.

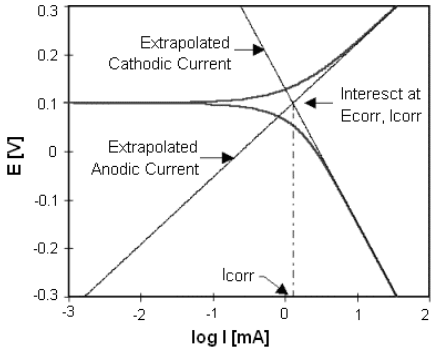


Fig. 1. Tafel curve analysis.

From the LP curves, the E_{corr} potential, the I_{corr} current and the R_p resistance parameters are determined. The I_{corr} current has been determined by drawing a straight line along the linear portion of the cathodic or anodic curve and by extrapolating it through E_{corr}. The corrosion rate (mm/y) was calculated from the following equation:

$$V_{corr}(mm/y) = \frac{0.051 \cdot I_{corr}(e.w.)}{A \cdot \rho} \quad (1)$$

where: *e.w.* is the equivalent weight (g/eq.), A is the area (cm^2) and ρ is the density (g/cm^3).

The polarization resistance is another important parameter for the characterization of the performance of anticorrosive properties of environments. The R_p resistance can be determined by using the Stearn-Geary equation, namely:

$$R_p = \frac{\beta_a \cdot \beta_c}{2.303 \cdot (\beta_a + \beta_c) \cdot I_{corr}} \quad (2)$$

where: β_a and β_c are the Tafel slopes $\Delta E / \Delta \log I$ for positive and negative domains of the Tafel curve as presented in Fig. 1.

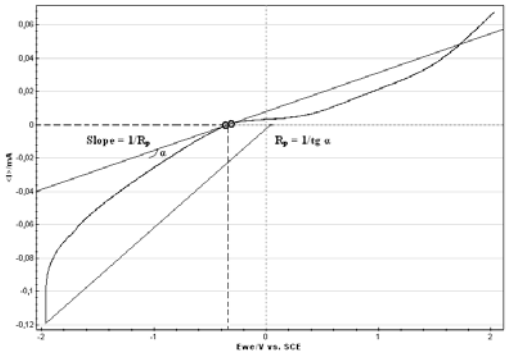


Fig. 2. How to calculate the polarization resistance.

Tafel curves were plotted by scanning the potential from – 1.15 to 1.13 V above the E_{corr} at a scan rate of 20 mV/s. The R_p was obtained from the slope of the potential-current plot as it can be seen in the Fig. 2 above [17,18].

3. Results and discussion

The 316L SS coins prepared as WE were chemically cleaned and rinsed with bi-distilled water before their immersion in the electrochemical cell. Five type of electrolyte solutions were tested during the corrosion experiments: demineralised and deionised water; 0.1 and 0.2 g/L TiO_2, respectively 0.1 and 0.2 g/L Al_2O_3. First, the rest potential was measured vs. SCE to stabilise the WE interface into the electrolyte during the OCP measurements. The OCP graphs (not shown) are recorded with a duration of 60 s to find the free (rest) potential. Then the corrosion processes were recorded by means of LP method [19]. The goal of this research was to evaluate the behaviour of SS disks in five different environments during three working times: 1, 2 and 4 min. Also, the pH values from the beginning to the end of the testing are determined.

The polarisation Tafel curves (Figs. 3÷10) obtained from LP measurements allow to determine some electrochemical parameters such as E_{corr}, I_{corr}, R_p and Tafel slopes (the slope of the tangent to the anodic branch – β_a – the oxidation reaction and the slope of the tangent to the cathodic branch – β_c –the reduction process). These parameters are calculated using the Tafel and R_p fit. analysis tools menu. Finally, the corrosion rate (V_{corr}) can be automatically calculated by means of the software using the equation (1). These parameters could be useful when referring to the surface corrosion resistance inside an environment. The results are shown in Figs. 3 to 10 and electrochemical parameters are summarized in Tables 2 to 6.

3.1. AISI 316L SS in demineralised and deionised water Tafel analysis

First, by means of a potentiodynamic polarization curve, it is investigated how the demineralised and deionised water (real medium), at 22÷25 °C, can affect the surface stability of the AISI 316L SS. During the OCP measurements (not shown), the free potential of metallic samples into the water was registered at E_1 = -17 mV.

Fig. 3 presents the variation of E_{corr} potential during the polarization of AISI 316L SS immersed in demineralised and deionised water at different exposure times. The E_{corr} potential was maintained at a constant value (-337 mV) in the negative range for each immersion time (see data from Table 2). By increasing exposure time (more than 4 min.), a slight shifting tendency towards positive range will be possible and then the 316L SS stability in contact with demineralised and deionised water is induced.

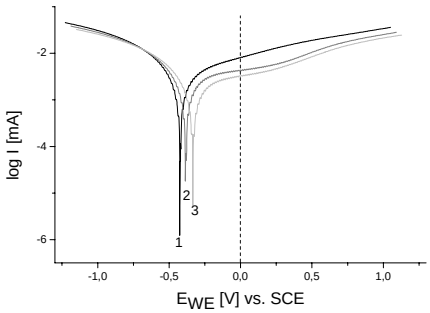


Fig. 3. Linear Polarization curves of 316L SS in the demineralised and deionised water environment at different immersion times: (1) 1 min; (2) 2 min and (3) 4 min.

The electrochemical parameters obtained at 316L SS/water interface as read from the potentiodynamic polarization curves are listed in Table 2. The I_{corr} current is constant (~ 1.18 μA) while the R_p resistance slightly increased. The V_{corr} rate indicates very low and constant values over time.

During these experiments the cathodic process has a linear shape, so there is no passivity reaction. For t_1 the anodic process is a simple exponential and the Tafel curve has a linear shape. However, for t_2 and t_3 the right side curves are nonlinear due to the oxide layer formation. By increasing time, the electrochemical passivation from anodic polarisation curves (t_2 and t_3 curves) increases. This

behaviour can be explained on the basis of inert action of this medium against disk-shaped substrates.

Table 2. Tafel and R_p fit. corrosion parameters of 316L SS under the action of demineralised and deionised water environment.

Water	AISI 316L Stainless Steel					
Time (min.)	E_{corr} [mV]	I_{corr} [μA]	β_c [mV]	β_a [mV]	V_{corr} [μm/y]	R_p [kΩ]
$t_1 = 1$	-340.52	1.17	275.4	402.9	0.73	40.79
$t_2 = 2$	-340.06	1.19	274.9	480.3	0.73	41.53
$t_3 = 4$	-331.41	1.17	267.4	520.3	0.72	42.77

The pH value was not changes during this test (pH = 5.7 is the normal pH value of demineralised and deionised water). The water is an acidic but non-aggressive environment due to the low corrosion rate values. These substrates are not corroded during these experiments. The electrical conductivity is a very important property used to check the purity of water. This environment is a very poor electrical conductive. The electrical conductivity value is 20 μS/cm. From the literature, it is known that the electrical conductivity of demineralised and deionised water varies between 1 and 1000 μS/cm. This fact means that very few numbers of metallic ions from substrates are reduced during the chemical reactions.

3.2. AISI 316L SS in 0.1 g/L TiO_2 suspension Tafel analysis

Two different TiO_2 nanoparticle suspensions (0.1 and 0.2 g/L) are prepared to evaluate the corrosion effect of these media upon the metallic substrates after the pre-treatment operations. Before starting the experiments these suspensions are ultrasound tested for 20 min. in order to cause an electrostatic charge to TiO_2 nanoparticles. The analysis times are 1, 2 and 4 min. using the LP method. The potential range was between (–1.15÷1.13) V vs. SCE. The free potential from the OCP measurement (not shown) for 0.1 g/L TiO_2 solution was performed at E_2 = -250 mV.

Fig. 4 shows the effect of the 0.1 g/L TiO_2 electrolyte solution against the button-shaped samples. By increasing immersion time, polarization curves are slightly shifted to more negative E_{corr} values (~ -207 mV). At t_1 the I_{corr} has a low value, but the R_p is very high and the solution seems to have an inert activity (Table 3). Then, by increasing immersion time, I_{corr} current and V_{corr} rate slightly increase and the R_p is drastically decreased. This fact can be due to the slightly electroactivity particles behaviour but not enough electron density through the solution to determine metal dissolution. The shift of E_{corr} suggests that the 0.1 g/L TiO_2 suspension is a possible depolarizing agent, confirmed by the predominant anodic Tafel slopes [20-22] as it can be seen in Table 3. β_a ranged between 278.9 and 379.1 mV [23].

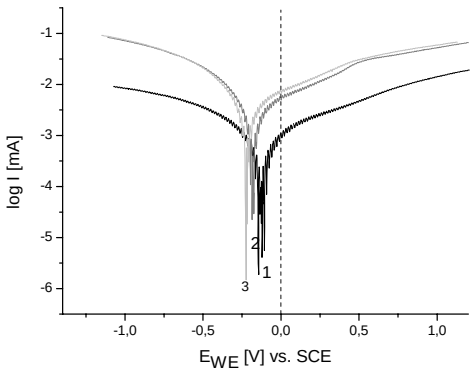


Fig. 4. Linear Polarization curves of 316L SS in the 0.1 g/L TiO_2 environment at different immersion times: (1) 1 min; (2) 2 min and (3) 4 min.

By decreasing R_p, working time increases. This observation indicates that the TiO_2 nanoparticle suspensions can produce the corrosion process, thus confirming by decreasing of corrosion rate values. At lower concentration (0.1 g/L) the TiO_2 environment is a little more aggressive than water and it can attack the metallic 316L SS surface. This fact can be due to the lower nanoparticle concentrations which are not enough to create a protective layer. Therefore the next solution will contain a double amount of TiO_2 nanoparticle suspensions.

Also, in this case, for each experiment, the Tafel cathodic and anodic branches are linear exponential curves. There is no oxide layer formation onto the AISI 316L SS surface.

Table 3. Tafel and R_p fit. corrosion parameters of 316L SS under the action of 0.1 g/L TiO_2 suspension.

	AISI 316L Stainless Steel					
Time (min.)	E_{corr} [mV]	I_{corr} [μA]	β_c [mV]	β_a [mV]	V_{corr} [μm/y]	R_p [kΩ]
$t_1 = 1$	-172.87	0.61	290.6	313.5	0.38	75.19
$t_2 = 2$	-214.15	2.04	260.8	402.3	1.26	23.32
$t_3 = 4$	-205.65	2.38	276.5	379.1	1.48	20.24

The pH value was not modified during the experiment (pH = 6.1) showing a poor acid working environment. Also, the electrical conductivity was constant at 20.2 μS/cm which is specific to water. The electrical activity of this test solution was not changed by adding 0.1 g/L TiO_2 nanoparticles. Therefore a few numbers of metallic ions were reduced during the corrosive processes.

3.3. AISI 316L SS in 0.2 g/L TiO_2 suspension Tafel analysis

The rest potential from OCP measurements (not shown) for 0.2 g/L TiO_2 solution was recorded at E_3 = -57 mV. Fig. 5 shows the effect of 0.2 g/L TiO_2 medium against the metallic cathode at three immersion times. The

E_{corr} potential is relatively constant and it has a slight tendency to go downward to the positive domain. From Table 4 the I_{corr} and V_{corr} values are higher with increasing immersion time in comparison with two previous electrolytes. This electrolyte has electroactive behaviour due to the I_{corr} increasing, and the electron number grows. Just like electrons in wires, these ions contribute to the transport charge in the electric field and thus to the current flow. In this situation the system responds by means of a predominant anodic current (Table 4) and it can accelerate the metal dissolution [23].

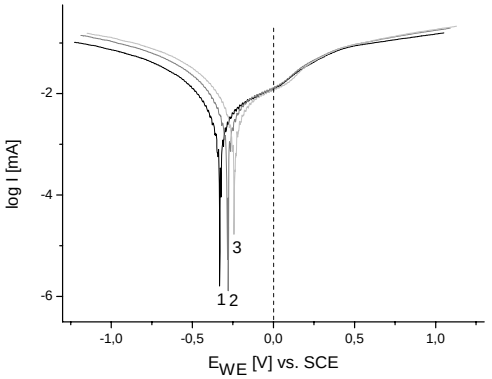


Fig. 5. Linear Polarization curves of 316L SS in the 0.2 g/L TiO_2 environment at different immersion times: (1) 1 min; (2) 2 min and (3) 4 min.

Also, the lower R_p resistance values indicate that the 0.2 g/L TiO_2 is a corrosive environment. One single passivity process for each exposure time occurred during the experiment. Thereby, a very small amount of TiO_2 particles could be enough to limit the corrosion phenomenon. The nonlinear polarization curves from Fig. 5 above (right side) show a passivity process occurring. This is possible due to the mass charge transfer limitation.

Table 4. Tafel and R_p fit. corrosion parameters of 316L SS under the action of 0.2 g/L TiO_2 suspension

	AISI 316L Stainless Steel					
Time (min.)	E_{corr} [mV]	I_{corr} [μA]	β_c [mV]	β_a [mV]	V_{corr} [μm/y]	R_p [kΩ]
$t_1 = 1$	-253.69	2.72	252.1	407.8	1.69	17.81
$t_2 = 2$	-248.71	3.49	241.5	431.0	2.17	13.80
$t_3 = 4$	-236.59	3.77	255.9	421.9	2.22	12.17

The pH was measured and it shows an almost neutral solution (pH = 6.5), but the electrical conductivity value is doubled (47 μS/cm). Thereby, a high number of metallic ions are reduced at the cathode surface. This phenomenon can be explained by the partial dissolution of Ti^{4+} ions from the electrolyte. The AISI 316L SS surface becomes inactive in the alkaline environment and thus the inability to form an oxide layer onto the surface.

In the electrochemical system the electrolytic hydrogen and oxygen ions occur. Therefore, there is a large electron flow which can cause a current increasing and different anodic and cathodic polarizations. This polarization is practically confirmed by the Tafel slopes (β_a and β_c) shifting [20-22]. As it can be seen from Table 4 this nanoparticle suspensions shifts the β_c slope from 251 to 256 mV and the β_a slope from 408 to 422 mV. The Tafel slopes shifting highlights that the TiO_2 suspension influenced the corrosion mechanism [24] and controlled mainly the anodic reactions. The shifting of E_{corr}, the increase of I_{corr} and decrease of R_p values indicate a synergist effect of the system formed by from demineralised and deionised water – 0.2 g/L TiO_2 nanoparticle suspensions – applied potential, thus confirming the increase of corrosion rate values of AISI 316L SS. This effect is developed by a predominant anodic current which can accelerate the corrosion process in this case.

3.4. AISI 316L SS in 0.1 g/L Al_2O_3 suspension Tafel analysis

Hereinafter, the TiO_2 nanoparticles are replaced with the inorganic Al_2O_3 nanoparticles for two concentrations in order to test the passivation capability of the button-shaped samples in these solutions. From the OCP measurement (not shown) the 316L SS rest potential recorded inside the 0.1 g/L Al_2O_3 medium was E_4 = -25 mV. Fig. 6 presents the current-potential response of AISI 316L SS immersed in Al_2O_3 suspensions during the polarization experiments.

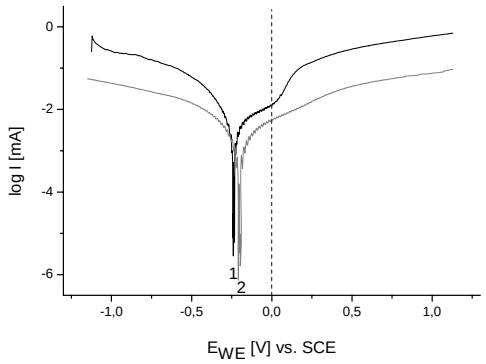


Fig. 6. Linear Polarization curves of 316L SS immersed in the 0.1 g/L Al_2O_3 environment at different immersion times: (1) 1 min; (2) 2 min and (3) 4 min.

By increasing working time, polarization curves can slightly shift to the positive range of the E_{corr} potential. Under these circumstances, the metallic substrates will become stable in this environment. A large range of passivation processes on both cathodic and anodic branches could be observed and an oxide layer formation onto the SS surface is possible. This is confirmed by the tripled R_p resistance values (Table 5). The 0.1 g/L Al_2O_3

solution limited the corrosion effect confirmed by the subunit corrosion rate values.

Table 5. Tafel and R_p fit. corrosion parameters of 316L SS under the action of 0.1 g/L Al_2O_3 suspension

	AISI 316L Stainless Steel					
Time (min.)	E_{corr} [mV]	I_{corr} [μA]	β_c [mV]	β_a [mV]	V_{corr} [μm/y]	R_p [kΩ]
$t_1 = 1$	-208.28	1.60	251.2	386.0	0.99	31.87
$t_2 = 2$	-191.50	1.66	281.6	344.5	0.98	27.35

The Al_2O_3 added in the electrolyte solution can change the suspension pH value. The pH was measured at 5.0 which is less than demineralised and deionised water pH. The electrical conductivity is 21.0 μS/cm and the electrolyte is a poor electrical conductive. This fact means that a very few number of metallic ions from substrates or from solutions are reduced during the electrochemical process.

3.5. AISI 316L SS in 0.2 g/L Al_2O_3 suspension Tafel analysis

The free potential from OCP measurements (not shown) for 0.2 g/L Al_2O_3 solution was recorded at E_5 = -6.5 mV. Fig. 7 indicates the current-potential dependence of SS immersed into the 0.2 g/L Al_2O_3 electrolyte solution. A nonlinear anodic branch shape highlights the passivity action of 316L SS which is confirmed by the slightly increasing values of R_p resistance.

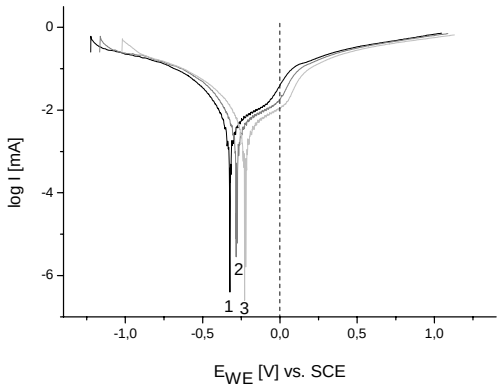


Fig. 7. Linear Polarization curves of 316L SS in the 0.2 g/L Al_2O_3 environment at different immersion times: (1) 1 min; (2) 2 min and (3) 4 min.

Table 6 shows the electrochemical parameters obtained for the system of 316L SS/0.2 g/L Al_2O_3 nanoparticle suspensions. The E_{corr} potential is performed only in the negative range at a constant value (~ -220 mV), result which is confirmed by the predominant anodic Tafel slopes. However, at exposures above 4 min, the potential will slowly increase towards positive values having a stability effect of 316L SS in this environment. By adding 0.2 g/L Al_2O_3, on the one hand, the data from Table 6 confirm the electroactive behaviour of the tested electrolyte solution and on the other hand, a high electron current. A high current is produced during 1 min. (Fig. 7, gray dark curve). But by increasing contact time (over 4 min.), the I_{corr} current slowly decreases due to the OH^- absorption [18,25]. Simultaneously, a partial surface passivation could occur.

Table 6. Tafel and R_p fit. corrosion parameters of 316L SS under the action of 0.2 g/L Al_2O_3 suspension.

	AISI 316L Stainless Steel					
Time (min.)	E_{corr} [mV]	I_{corr} [μA]	β_c [mV]	β_a [mV]	V_{corr} [μm/y]	R_p [kΩ]
$t_1 = 1$	-225.10	4.37	212.4	435.9	2.72	9.30
$t_2 = 2$	-222.96	4.26	210.9	451.1	2.64	9.45
$t_3 = 4$	-202.18	3.90	232.7	432.6	2.41	11.91

The pH value was not modified during this experiment (pH = 5.0) showing a poor acid working environment. The electrical activity of this test solution was changed by adding 0.2 g/L Al_2O_3 nanoparticles (16.40 μS/cm). This value is specific to demineralised and distilled water. As said above, by increasing exposure time, a poor electrical activity can be performed. From the literature it is known that the optimal coatings are taken especially in very acidic media [5-7] and 316L SS has a good corrosion resistance. The Al^{3+} and Ti^{4+} ions inhibit the H^+ evolution from cathodic reaction developing a protective oxide layer. Therefore, by increasing Al_2O_3 nanoparticle concentrations and exposure time, solution could limit the corrosion phenomenon. The Al_2O_3 coatings allow using the AISI 316L SS or other composite materials based on AISI 316L SS in different kinds of applications and tests.

3.6. The synergistic effect of working parameters

Fig. 8 shows the R_p values of AISI 316L SS immersed in all electrolyte solutions, at different exposure times.

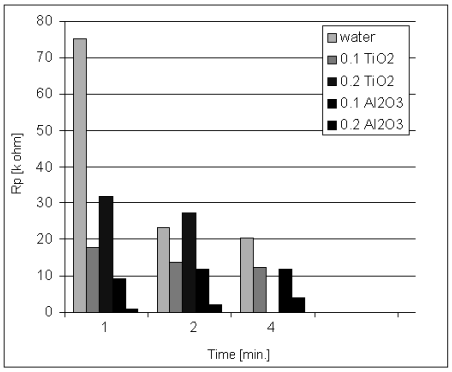


Fig. 8. Polarisation resistance of 316L SS immersed in different environments at different exposure times.

The R_p values are lower in the electrolyte solutions in comparison with them in the reference medium. The disk-shaped metallic samples present a higher surface

resistance in the 0.2 g/L TiO_2 unlike the other one suspension which contains a half TiO_2 concentration.

Concerning the Al_2O_3 nanoparticle suspensions the one which contains 0.1 g/L demonstrate good resistance to stainless steel corrosion. The nanoparticle concentrations from the suspension are reduced, the metallic surface resistance is more.

The obtained results suggest that the AISI 316 L metallic surfaces is more susceptible in the electrochemical systems which contain mixed solution: demineralised and deionised water with addition of nanoparticle suspensions (0.1 and 0.2 g/L).

The corrosion is a complex phenomenon which depends on the composition and structure of the metallic material, the nature and composition of the corrosive environment and the conditions in which the reactions take place.

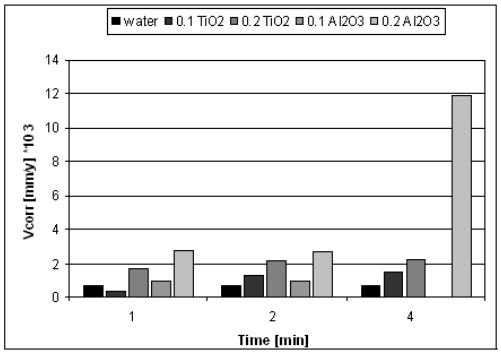


Fig. 9. Corrosion rate of 316L SS immersed in different environments at different exposure times.

Fig. 9 presents the corrosion rate evolution of AISI 316L SS immersed in various environments at different times. The demineralised and deionised water environment corrodes very slowly and at the constant values.

There can be observed that the V_{corr} values are higher by immersion in the mixed solutions in comparison with water-reference medium and increasing the exposure time. By studying the obtained results, the relatively high V_{corr} rates during the corrosive experiment in 0.1 and 0.2 g/L TiO_2 and Al_2O_3, respectively can detect in few exposure minutes; then the corrosion rates intensify at the end of the measurement. This fact suggests that there is no electrochemical performance for AISI 316L SS immersed in mixed solution.

The obtained information suggests that the insoluble corrosion products are formed onto the metallic surface (protective layers) but they become soluble at the end of experiment (the measurements were performed under static conditions).

3.7. AISI 316L SS in different suspensions Tafel analysis

The electrochemical behaviour of these five systems can be compared simultaneously at three different immersion times through the electrochemical parameters obtained by means of Tafel fit. and R_p fit. analysis tools menu as well as graphically by viewing the polarization curves. The electrochemical parameters, specified above, are useful to obtain the information about their metallic surfaces resistance inside the environment.

Fig. 10 shows the E_{corr} potential values obtained during the 316L SS polarization exposed to different electrolyte solutions for 1 min. The E_{corr} vs. I_{corr} diagram (Fig. 10, curves 1÷5) indicates that E_{corr} potential values are negative for all five tested solutions. The important corrosion parameters (R_p and V_{corr}) come out from Tables from 2 to 6.

The E_{corr} potential and I_{corr} current are -340.52 mV and 1.17 μA, respectively in demineralised and deionised water; -172.87 mV and 0.61 μA, respectively in 0.1 g/L TiO_2 suspension; -253.69 mV and 2.72 μA, respectively in 0.2 g/L TiO_2 suspension; -208.28mV and 1.60 μA, respectively in 0.1 g/L Al_2O_3 suspension and -225.10 mV and 4.37 μA, respectively in 0.2 g/L Al_2O_3 suspension (Tables 2 to 6). These data demonstrate that the electrochemical system which contains nanoparticle suspensions (0.2 g/L Al_2O_3 (curve 5), particularly) is characterized by a high electron density (I_{corr}) which is direct proportional with the concentration. Thereby, the current intensity passing through the suspension is higher than that from the water-reference environment due to the addition of nanoparticle suspensions. Also, the lower current value (0.61 μA) suggests a higher 316L SS resistance (75.19 kΩ) against the 0.1 g/L TiO_2 nanoparticle suspensions. This fact could be explained by the SS composition and size of (nano)particles.

Also, the E_{corr} potential variation at successive scanning potential of the WE immersed in the solutions could be observed.

The absence of the anodic and cathodic branches parallelism between the curves 2÷5 (nanoparticle suspensions) and the curve 1 (water-reference medium) represents a dissimilar character of the processes occurred onto the AISI 316 surface during immersion [25].

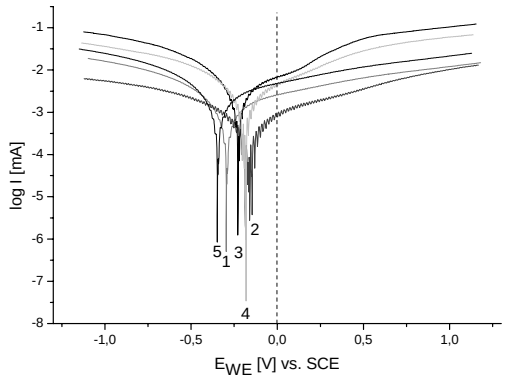


Fig. 10. Linear Polarization curves of 316L SS in different environments for 1 min: (1) demineralised and deionised water; (2) 0.1 g/L TiO_2; (3) 0.2 g/L TiO_2; (4) 0.1 g/L Al_2O_3 and (5) 0.2 g/L Al_2O_3.

The E_{corr} potential variation as a function of I_{corr} current is presented in Fig. 11 where the corrosion potential values are recorded in the negative range for a 2 min immersion time. But the E_{corr} value is more negative for AISI 316L SS exposed in water-reference solution (-340.06 mV) and the lower corrosion current (1.19 μA) involves the higher polarisation resistance (41.53 kΩ).

Also, at first scanning electrode potential a displacing in negative range can be observed with an amplitude of almost 126 mV. After that, at the following scanning potentials the corrosion potential slightly refines by shifting to the positive domain with an amplitude which becomes smaller (~ 3 mV) at the end of test.

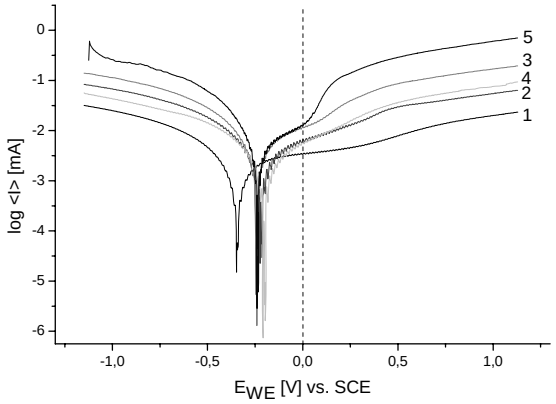


Fig. 11. Linear Polarization curves of 316L SS in different environments for 2 min: (1) demineralised and deionised water; (2) 0.1 g/L TiO_2; (3) 0.2 g/L TiO_2; (4) 0.1 g/L Al_2O_3 and (5) 0.2 g/L Al_2O_3.

Then, by adding nanoparticles, a potential displacing to the positive range and a chemical stability can occur (the E_{corr} is relatively constant). Also, there are no similar cathodic and anodic processes because of the different red-ox reactions occurred. By increasing immersion time, polarisation resistance decreases.

Finally, the last testing takes 4 min. to evaluate the modification of corrosion potential vs. corrosion current. Fig. 12 shows a corrosion potential and current evolution during the AISI 316L SS polarization immersed in different electrolyte solutions for 4 min. From the LP curves it can observed that the E_{corr} values are in the negative range with a slightly tendency to move to the positive values for the suspensions.

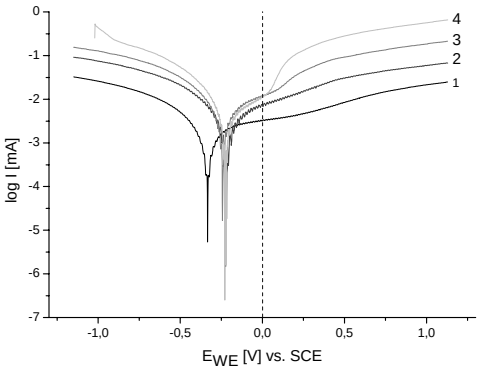


Fig. 12. Linear Polarization curves of 316L SS in different environments for 4 min: (1) demineralised and deionised water; (2) 0.1 g/L TiO_2; (3) 0.2 g/L TiO_2; (4) 0.1 g/L Al_2O_3 and (5) 0.2 g/L Al_2O_3.

Tables 2 to 6 present the electrochemical parameters which are specific to AISI 316L SS. By increasing immersion time, the corrosion rate increases being constant at the end. This variation is due to some factors such as the electrolyte type, applied scanning potential, exposure time and substrate composition. In accordance with the data from the tables above, once again, the higher electron density is characteristic to the electrochemical systems which contain only 0.2 g/L TiO_2 and Al_2O_3, respectively suspensions. This indicates a great sensitivity of disk-shaped metallic samples to the nanoparticle suspensions [18,25]. This sensitivity is associated with the higher corrosion rate.

4. Conclusions

From the obtained results of both polarization-based measurement methods (Tafel slopes extrapolation and polarization resistance) of the AISI 316L Stainless Steel exposed to various aqueous environments it may be concluded that:

The corrosion process and electrochemical parameters depend on some factors: electrolyte type, exposure time, pH value, chemical composition of working electrode, applied scanning potential and particles concentration and size.

At 22-25 °C demineralised and deionised water does not cause a corrosion process at the steel surface even without any surface pre-treatment.

By increasing exposure time, the electrochemical passivation from anodic polarisation curves developed. After passivation the corrosion rate will diminish and polarisation resistance increases.

The 0.1 g/L TiO_2 nanoparticles suspension is the lower corrosive environment for stainless steel with a higher resistance surface for a short exposure time (1 min.). By increasing immersion time (over 4 min.), the most stable electrochemical system is demineralised and deionised water.

The 0.2 g/L TiO_2 nanoparticles suspension is a corrosive environment showing a lower polarization resistance. Thereby, a very small amount of TiO_2 nanoparticles could be enough to limit the corrosion phenomenon.

The higher corrosion rate was found at 0.2 g/L Al_2O_3 suspension in an acidic environment. By increasing working time, this medium can limit the corrosion process by hydrogen ions evolution inhibition.

The obtained results suggest that the AISI 316 L metallic surfaces is more susceptible in the electrochemical systems which contain mixed solution: demineralised and deionised water with addition of nanoparticles suspension (0.1 and 0.2 g/L).

The nanoparticles concentration from the suspension is reduced, the metallic surface resistance is more.

There is no electrochemical performance for AISI 316L SS immersed in mixed solution concerning the increasing of corrosion rate values.

The destructive action shown in these experiments could be determined by the chemical reactions occurred as a result of electric currents passing through the liquid environment.

References

[1] R. A. Lula, Stainless Steel, American Society for Metals, Metals Park Press, Ohio (1986).
[2] S. Kožuh, M. Gojić, Zavarivanje **49**(5), 177 (2006).
[3] M. Gojić, M. Dražen, M. Tudja, S. Kožuh, RMZ – M&G **55**(4), 408 (2008).
[4] M. V. Regi, I. I. Barba, F. J. Gil, J. Biomed. Mater. Res. **67**A, 674 (2003).
[5] A. M. Cantaragiu, P. Cojocaru, L. Magagnin, G. Cârâc, C. Gheorghieş, J. Optoel. Adv. Mater. **12**(4) 913 (2010).
[6] J. Georgieva, S. Armyanov, E. Valova, I. Poulios, S. Sotiropoulos, Electroch. Acta **51**, 2076 (2006).
[7] S. A. Kumar, P. H. Lo, S. M. Chen, Nanotechnology **19**, 255501 (2008).
[8] G. E. Badea, A. Caraban, M. Sebesan, S. Dzitac, P. Cret, A. Setel, J. Sustain. Energ. **1**(1) (2010).
[9] T. Badea, M. Popa, M. Nicola, The Corrosion Sciences and Engineering, Romanian Academy Press, Bucharest (2002).
[10] N. Perez, Electrochemistry and Corrosion Science, Kluwer Academic Publishers Press, Boston (2004).
[11] R. G. Kelly, J. R. Scully, D. W. Shoesmith, R.G. Buchneit, Electrochemical Techniques in Corrosion Science and Engineering, Marcel Dekker Inc. Press, New York (2003).
[12] R. W. Rive, H. H. Uhlig, Corrosion and Corrosion Control. An Introduction in Corrosion Science and Engineering, J. Wiley & Sons Press, New Jersey (2008).
[13] P.R. Roberge, Corrosion Engineering. Principle and Practice, McGraw-Hill Press, New York (2008).
[14] S.M.A. Shibli, A.C. Jayalekshmi, Appl. Surf. Sci. **254**, 4103 (2008).
[15] G 5-94, ASTM, Easton, 55 (1997).
[16] G 1-90, ASTM, Easton, 15 (1997).
[17] C. Gheorghieş, L. Gheorghieş, C. Oancea, P. Hagioglu, V.O. Atanasiu, The Annals of "Dunarea de Jos" University of Galati, Fascicle IX, Metallurgy and Materials Science **2**, 38 (2009).
[18] M. Stoica, G. Cârâc, C. Tofan, O.E. Constantin, G. Enache, J. Agroal. Process. Techn. **15**(4), 543 (2009).
[19] B. Normand, C. Cabrillac, J. Crousier, J. J. Rameau, Rev. Métall. **9**, 689 (2002).
[20] G. T. Burstein, Corr. Sci. **47**(12) 2858 (2005).
[21] B. Elsener, Corr. Sci. **47**(12) 3019 (2005).
[22] E. McCafferty, Corr. Sci. **47**(12) 3202 (2005).
[23] M. Stoica, P. Popa, G. Cârâc, Proc. Eurocorr, Euro. Corr. Cong., Nice, France, 2009.
[24] B. M. A. Muhamath, K. Kulanthai, J. Appl. Sci. Environ. Manag. **13**(1) 27 (2009).
[25] M. Stoica, G. Cârâc, C. Apetrei, A.M. Cantaragiu, J. Optoelectron. Adv. Mater. **12**(35), 919 (2010).

* Corresponding author: cantaragiu_alina@yahoo.com